Chapter 6

Approach to Diagnosis of Salivary Gland Disease from Nuclear Medicine Images

Michihiro Nakayama, Atsutaka Okizaki,
Kaori Nakajima and Koji Takahashi

Additional information is available at the end of the chapter

http://dx.doi.org/10.5772/intechopen.70622

Abstract

Nuclear medicine images can help in the diagnosis and assessment of some salivary disorders. 99mTcO4−, gallium-67-citrate scintigraphy will be an indication of the function of salivary gland together and it will be used for the diffuse diseases such as sialadenitis, Sjögren's syndrome, sarcoidosis, glossopharyngeal paralysis, and irradiation. It is also effective for distinguishing benign tumor legion with Warthin's tumor and others. Moreover, fluorodeoxyglucose positron emission tomography (FDG-PET) is an indispensable modality for determining the localization, focal lesions, and staging of many malignant tumors, the fluorodeoxyglucose (FDG) accumulation is visually and semiquantitatively assessed using the standardized uptake value (SUV), which is the ratio of uptake to the injected dose per unit body weight. Also for radioactive iodine therapy, attention should be paid to adverse reactions. It is important to note that acute/chronic salivary gland disorders are associated with radioiodine therapy for the treatment of postoperative thyroid cancer. Coordination among healthcare providers including nurses, radiological technologists, and doctors of all departments involved in treatment is important for achieving effective outcomes.

Keywords: scintigraphy, 99mTcO4−, SPECT, FDG-PET, salivary gland disorders

1. Introduction

Radionuclide imaging, commonly used for the diagnosis of salivary gland diseases, consists of salivary scintigraphy using 99mTcO4−, gallium-67-citrate (67Ga) scintigraphy in inflammation, and fluorodeoxyglucose positron emission tomography (FDG-PET). It is important to note that acute/chronic salivary gland disorders are associated with radioiodine therapy for the treatment of postoperative thyroid cancer.

2. Salivary gland scintigraphy

2.1. Mechanism of uptake

Salivary glands secrete saliva. The parotid, submandibular, and sublingual glands are called the "major salivary glands." Salivary epithelial cells have a sodium/iodide symporter (NIS), which takes up univalent anions such as Cl− and I− and concentrates them (**Figure 1**). The concentrated anion is secreted into saliva. Administered 99mTcO4− (**Figure 2**) is taken up by the salivary glands through NIS, similar to Cl−. Thus, intravenously administered 99mTcO4− accumulates mainly in the parotid and submandibular glands and is excreted into saliva [1]. After the accumulation of the radionuclide, loading of citric acid, such as lemon juice, stimulates the secretion of saliva, which indicates salivary gland function. Salivary gland scintigraphy is useful for differentiating salivary gland tumors because Warthin's tumors and oncocytomas, which are benign, retain 99mTcO4−.

2.2. Testing procedure

Because salivary gland function is affected by food intake, 1 hour of fasting is needed before testing.

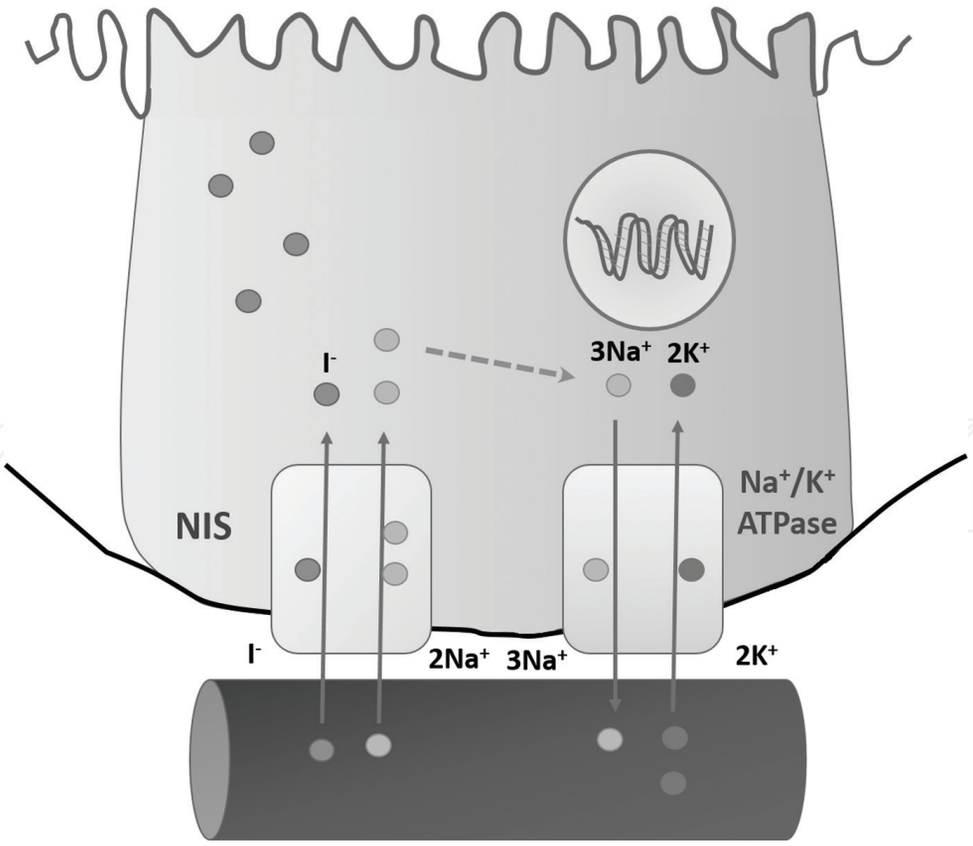

Figure 1. Iodide uptake mechanism of sodium/iodide symporter. Sodium/iodide symporter transports two sodium ions and one iodide ion into the cytoplasm together.

http://dx.doi.org/10.5772/intechopen.70622

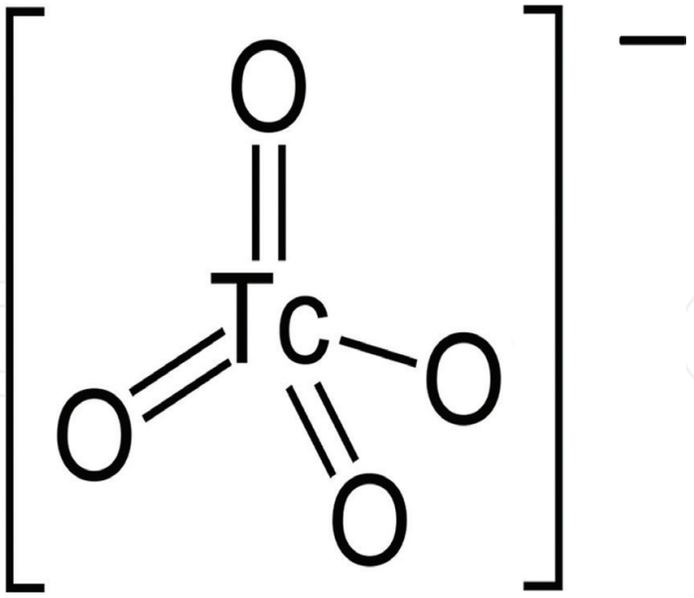

Figure 2. Structural formula of 99mTcO4−. 99mTcO4− is incorporated into the salivary glands through NIS, similar to Cl−.

For the kinetic analysis of salivary gland function, 185–370 MBq (5–10 mCi) of 99mTcO4− is intravenously administered. A dynamic scan (anteroposterior view) is performed at 5-minute intervals for 30 minutes. The thyroid gland should be included in the area. Citric acid (e.g., lemon juice) is instilled into the oral cavity 20 minutes after the intravenous injection to stimulate the secretion of saliva. The regions of interest are set at the bilateral parotid and submandibular glands, and at background regions to generate time-activity curves (TAC). The TAC is used to determine the function of individual salivary gland. For the diagnosis of tumors and morphology of salivary glands, the intravenously administered dose is 370–740 MBq, and the anteroposterior and lateral images are obtained 10–15 minutes after intravenous administration (**Figure 3**). When the assessment of the tumor is difficult due to the physiologic uptake in the normal salivary glands, washout by stimulating the secretion of saliva is useful.

2.3. Imaging evaluation

2.3.1. Normal images

Salivary gland scintigraphy provides information about the morphology and function of the salivary glands and the procedure is easier than that of sialography.

2.3.2. Dynamic scans and TAC

The uptake in the bilateral parotid and submandibular glands begins less than 1 minute after intravenous administration of the radionuclide and increases over time. The uptake in the parotid glands is equal to or greater than that in the submandibular glands. The sublingual glands are not visible, though the reason is unknown. After the stimulation of saliva secretion, the uptake rapidly declines in all four glands and subsequently rises again. The percentage

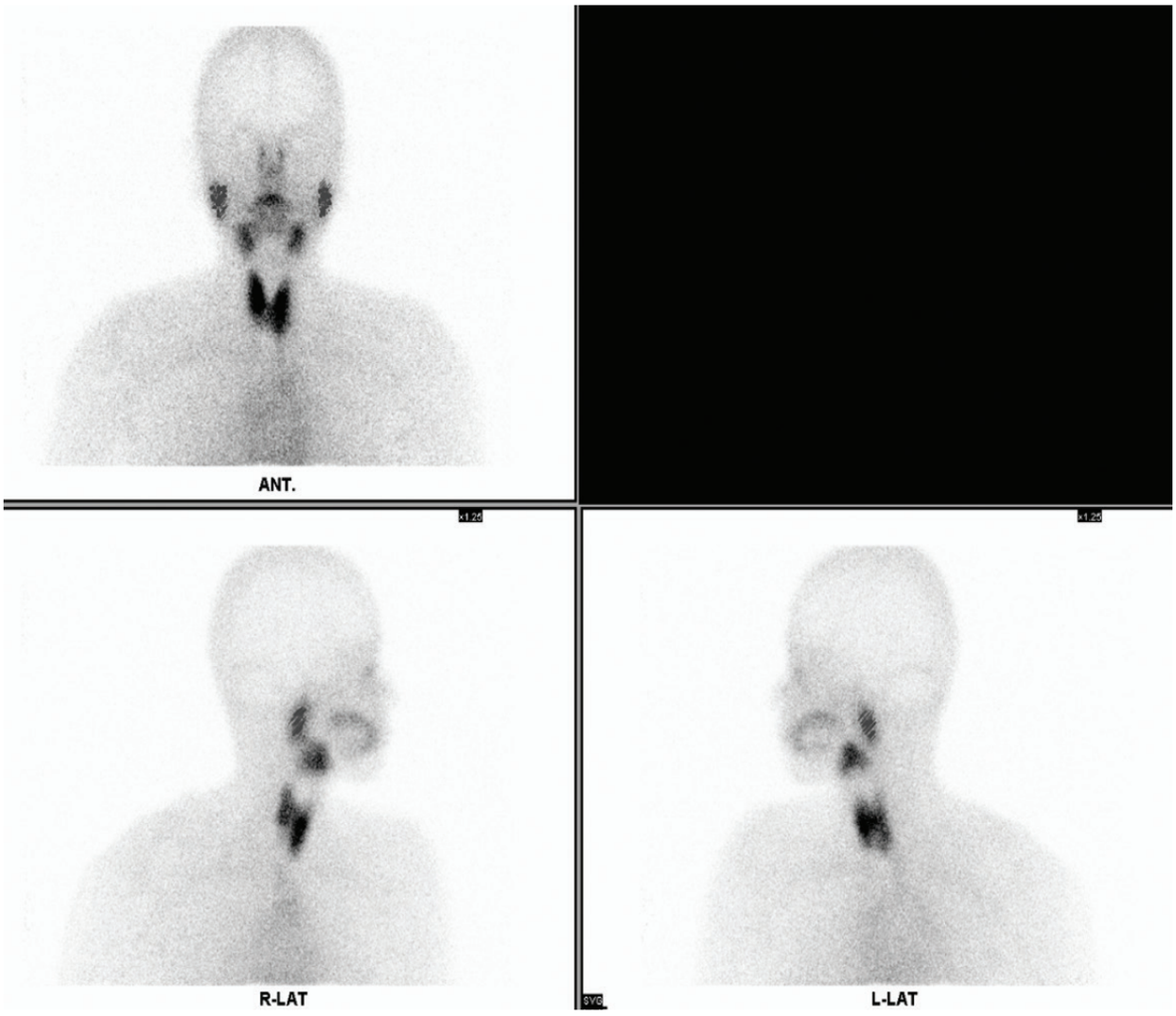

Figure 3. Static images in normal case. The radionuclide uptake of the parotid and submandibular glands is equal to or lower than that of the normal thyroid gland.

of washout is calculated using the counts at the maximum uptake and those at the minimum uptake seen after the stimulation of saliva secretion in each gland. The washout (%) is 50% or higher in the normal salivary gland (**Figure 4**).

2.3.3. Static images

The radionuclide uptake of the parotid and submandibular glands are equal to or lower than that of the normal thyroid gland, and mild uptake appears in the nasal and oral cavities. On the lateral view, the parotid gland is clearly shown, but the submandibular gland overlaps with the contralateral submandibular gland.

2.4. Diagnosis of salivary gland tumors

Warthin's tumors and oncocytomas are derived from the epithelial cells of excretory ducts and do not communicate via excretory ducts (**Figure 5**). Thus, 99mTcO4− is taken up by the

http://dx.doi.org/10.5772/intechopen.70622

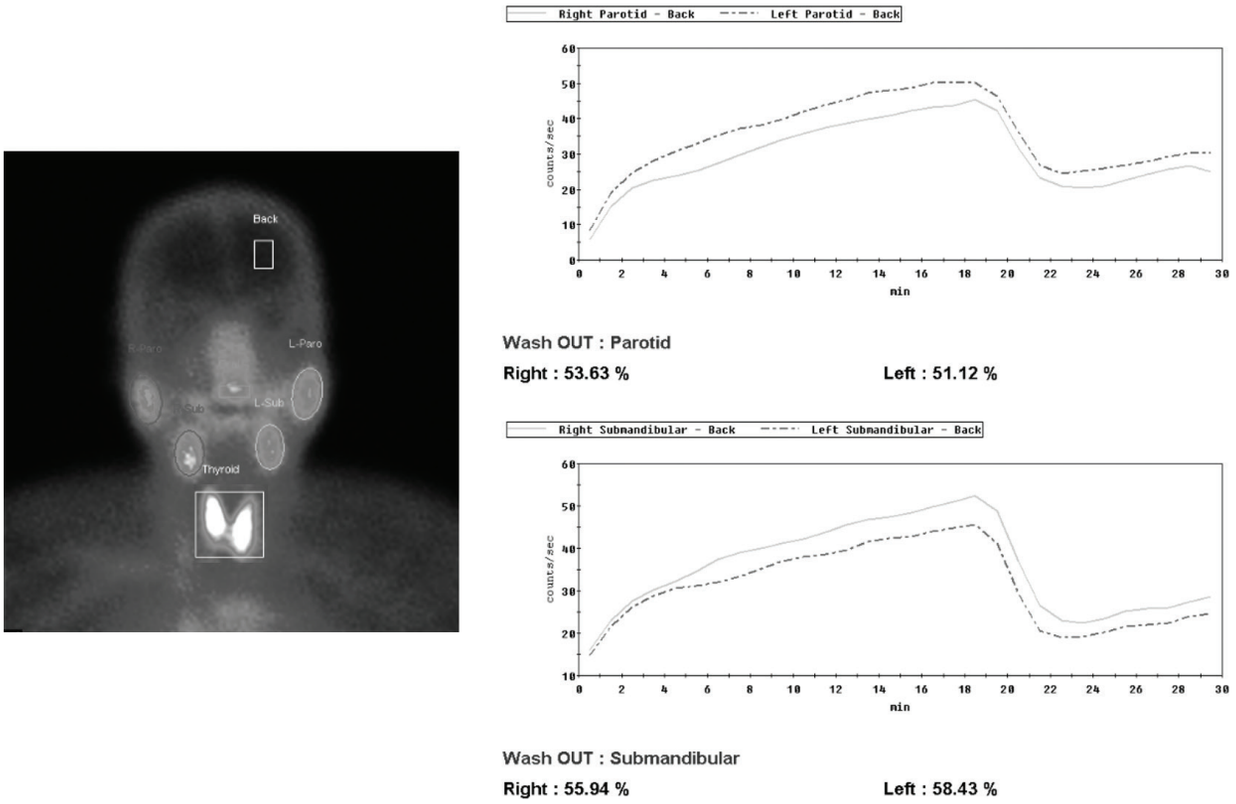

Figure 4. TAC of the normal salivary gland. After intravenous administration of the radionuclide, uptake in the parotid and submandibular glands increases over time. At 20 minutes after administration, saliva secretion is stimulated. Counts in the salivary glands rapidly decline and then gradually increase again.

solid component of these tumors and is not eliminated after the stimulation of saliva secretion. However, the uptake may be reduced in Warthin's tumor mainly with a cystic component. The diagnostic accuracy of salivary gland scintigraphy for Warthin's tumors and oncocytomas is around 90%, but these cannot be differentiated in salivary gland scintigraphy. Because Warthin's tumors develop bilaterally in 5–20% of cases, the contralateral parotid gland should be carefully evaluated. Meanwhile, because 99mTcO4− is not taken up by pleomorphic adenomas or parotid gland cancer (defect images), salivary gland scintigraphy is useful for differentiation [2].

2.5. Kinetic analysis of salivary gland function

The indications for kinetic analysis of salivary gland function include Sjögren's syndrome, acute/chronic sialadenitis, and facial/glossopharyngeal nerve palsy. Salivary gland function is assessed based on dynamic images and TAC. In general, chronic sialadenitis shows a decreased uptake while acute sialadenitis shows an increased uptake; acute/chronic sialadenitis shows a reduced or no response to stimulation of saliva secretion. Uptake in salivary glands is barely evident in patients with severe Sjögren's syndrome (**Figures 6** and **7**). The severity of the reduction in washout after the stimulation of saliva secretion well correlates with the results of the Saxon test. Thus, kinetic analysis reflects the severity of Sjögren's syndrome, allowing an objective assessment of salivary gland function [3].

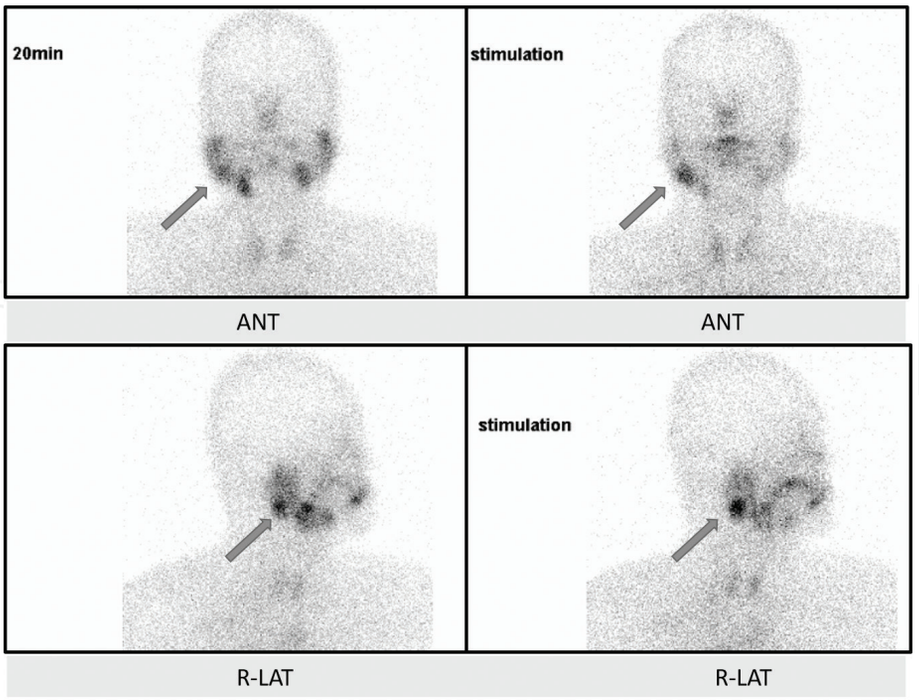

Figure 5. Warthin's tumor. On the image 20 minutes after administration, the radionuclide is taken up by the right parotid gland. After the stimulation of saliva secretion, the radionuclide remains in the right parotid tumor. The diagnosis was Warthin's tumor.

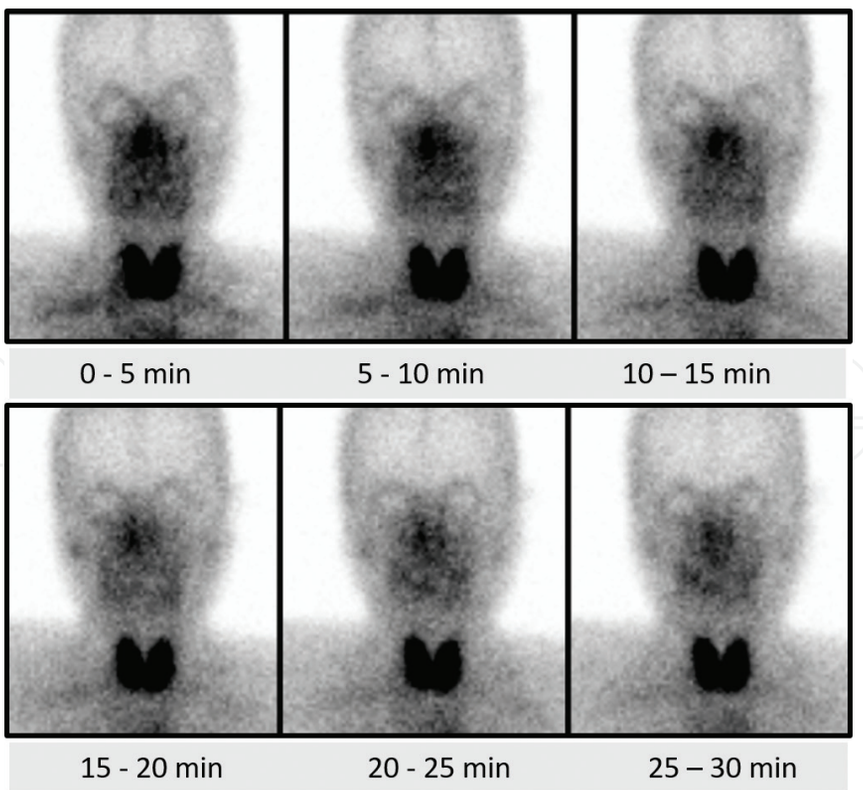

Figure 6. Sjögren's syndrome. All four salivary glands show decreased uptake.

http://dx.doi.org/10.5772/intechopen.70622

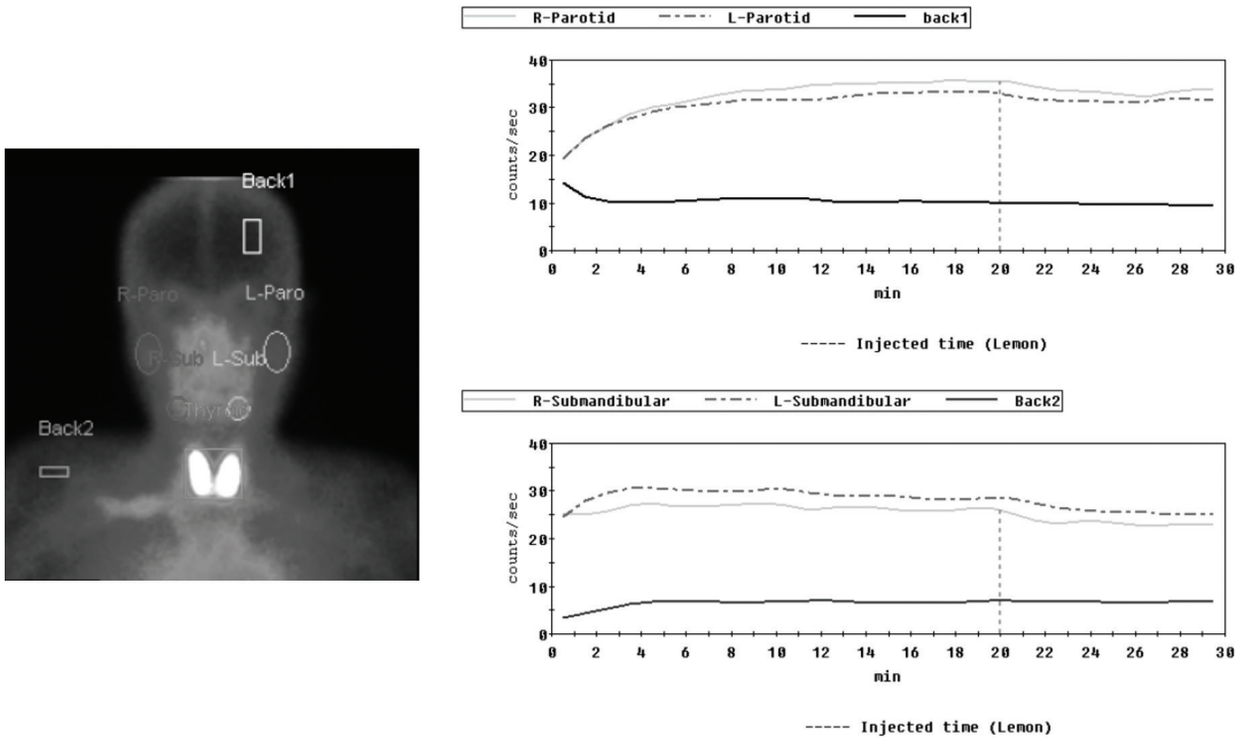

Figure 7. TAC of the Sjögren's syndrome. All four salivary glands show decreased uptake and a poor response to stimulation of saliva secretion 20 minutes after administration. TAC is useful for assessment.

3. Scintigraphy of inflammation (67Ga scintigraphy)

3.1. Mechanism of uptake

67Ga administered intravenously binds to transferrin, a serum protein, and is transported into cells through transferrin receptors. The carbon atom of citrate stabilizes the bond between 67Ga and transferrin. Transferrin receptors that bind to 67Ga distributed in lysosomes and cytoplasm are often present in tumor and inflammatory cells, which show intense uptake of 67Ga.

3.2. Testing procedure and imaging evaluation

67Ga is intravenously administered at a dose of 185–555 MBq. Imaging is performed 48–72 hours after intravenous administration to visualize the distribution of the radionuclide. 67Ga is excreted from the kidney and intestinal tract within 24 hours after administration and is mainly excreted by the liver. Intense uptake of 67Ga is noted in the liver, bone, and spleen 48–72 hours after administration. 67Ga is known to be taken up by inflammation and tumors; however, the sensitivity of 67Ga scintigraphy is low for malignant tumors, while the negative predictive value is high. Thus, a negative finding of focal uptake is likely to represent a benign lesion or low-grade tumor. Focal uptake in the parotid gland on 67Ga scintigraphy is useful for the supplemental diagnosis of Warthin's tumor. Meanwhile, with increased diffuse bilateral uptake, differential diagnosis includes sarcoidosis (**Figure 8**),

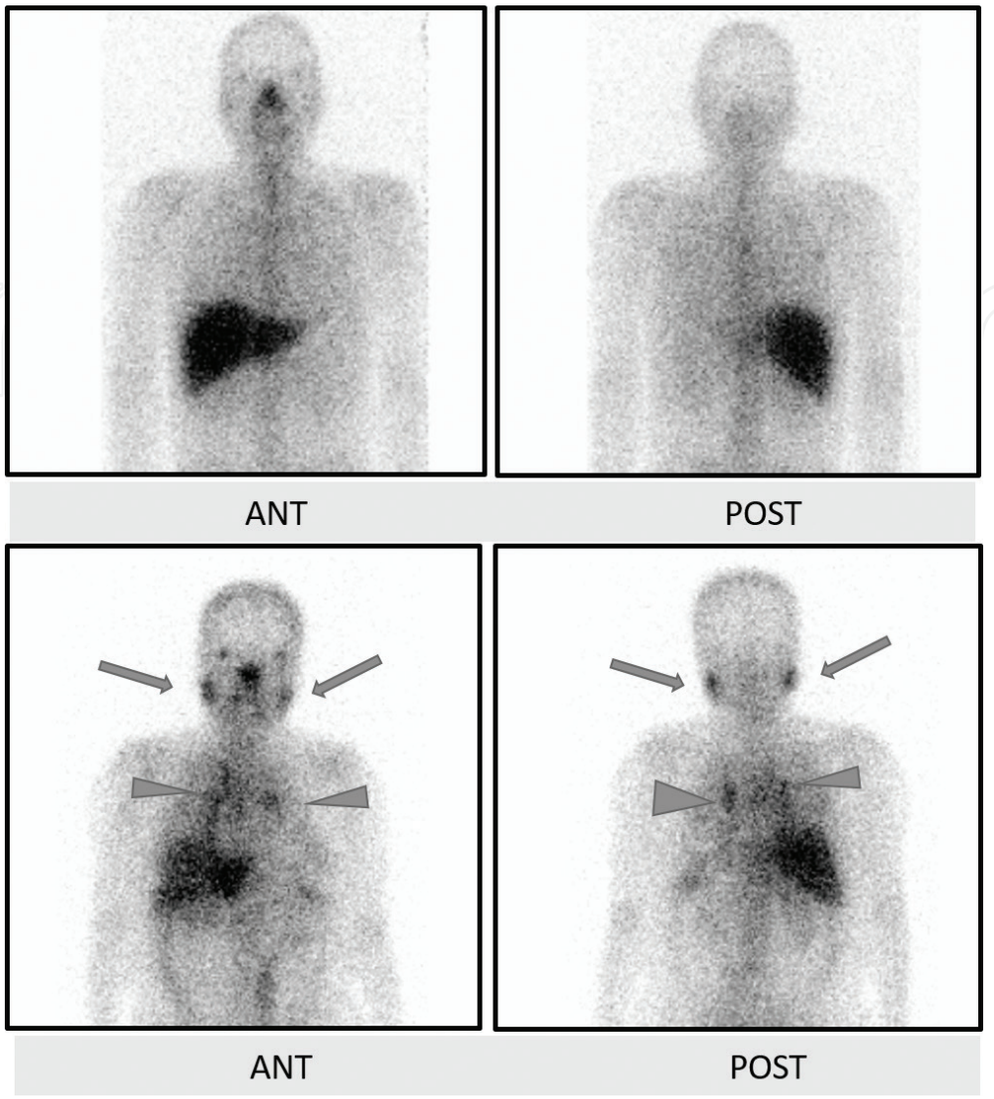

Figure 8. 67Ga scintigraphy. Upper column, normal image; lower column, sarcoidosis. Uptake is noted in the bilateral parotid glands (arrow), and mediastinal/hilar lymph nodes (arrowhead).

IgG4-related disease, Sjögren's syndrome, and Mikulicz disease. In recent years, 67Ga scintigraphy for tumor diagnosis has been increasingly replaced by FDG-PET, as described below.

4. PET

4.1. Mechanism of uptake

FDG-PET is a critical modality for determining the localization, focal lesions, and staging of many malignant tumors, as well as for their follow-up observation. It is also essential for the clinical management of salivary tumors [4–8]. Like glucose, fluorodeoxyglucose (FDG)

http://dx.doi.org/10.5772/intechopen.70622

is taken up by cells via glucose transporters and phosphorylated; however, unlike glucose, FDG remains in cells after phosphorylation. In general, glucose transporters and glucose metabolism are increased in tumor cells, leading to an increased uptake of FDG (**Figure 9**). The widespread use of PET combined with computed tomography (PET/CT) has increased the diagnostic accuracy by compensating for PET disadvantages, including poor spatial resolution and lack of anatomic information. Moreover, PET combined with magnetic resonance imaging (PET/MRI) has recently emerged.

4.2. Testing procedure

Fasting is required for 4 hours before testing and intake of liquids with sugar content is prohibited. FDG (**Figure 10**) is intravenously administered at a dose of 185–444 MBq (5–12 mCi). Imaging is performed 60–90 minutes after administration to visualize distribution. The accumulation is visually and semi-quantitatively assessed using the standardized uptake value (SUV), which is the ratio of uptake to the injected dose per unit body weight.

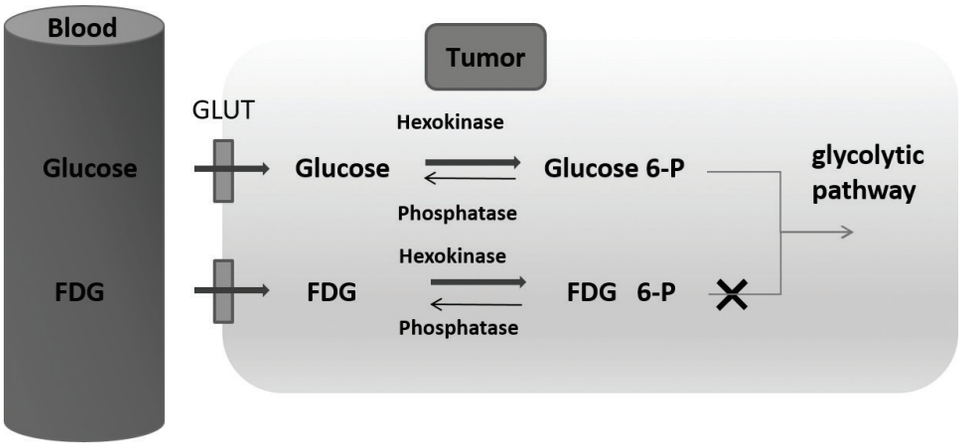

Figure 9. Mechanism of FDG uptake. Like glucose, FDG is taken up by cells via glucose transporters and phosphorylated; however, unlike glucose, FDG remains in cells after phosphorylation.

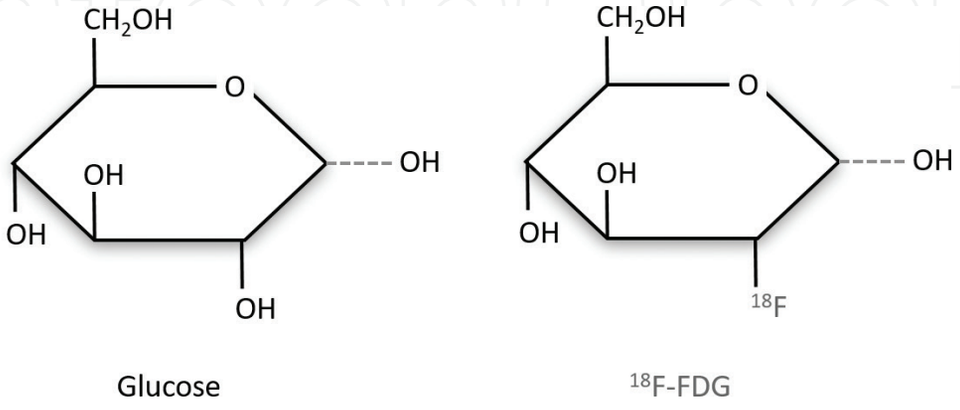

Figure 10. The chemical structure of FDG. The chemical structure of FDG is identical to that of 18F (one of the hydroxy groups of glucose that is replaced by a positron-emitting radionuclide).

4.3. Normal uptake

In the head and neck areas, many structures show physiologic uptake, including salivary glands, nasal and sinonasal mucosa, extraocular muscles, and lymphoid tissue. Because artifacts due to dentures are also often seen, information on CT or MRI images is useful [8].

4.4. Diagnosis of salivary gland tumors

Some lesions are difficult to differentiate from normal structures, postoperative changes, and inflammatory changes on CT or MRI images alone. However, those lesions can be diagnosed through the combined use of FDG-PET [4, 5, 7]. FDG-PET for medical evaluation or staging of a malignant tumor may incidentally reveal a salivary gland tumor [7, 9].

The differentiation of benign from malignant parotid tumors is difficult based on the results of FDG uptake alone. Moreover, the differentiation of benign from malignant salivary tumors is often difficult based on the comparison of the results of SUVmax alone. A malignant tumor tends to show more intense FDG uptake than a benign tumor; however, benign tumors, such as Warthin's tumor and pleomorphic adenoma (**Figure 11**) [10–12], also show high FDG

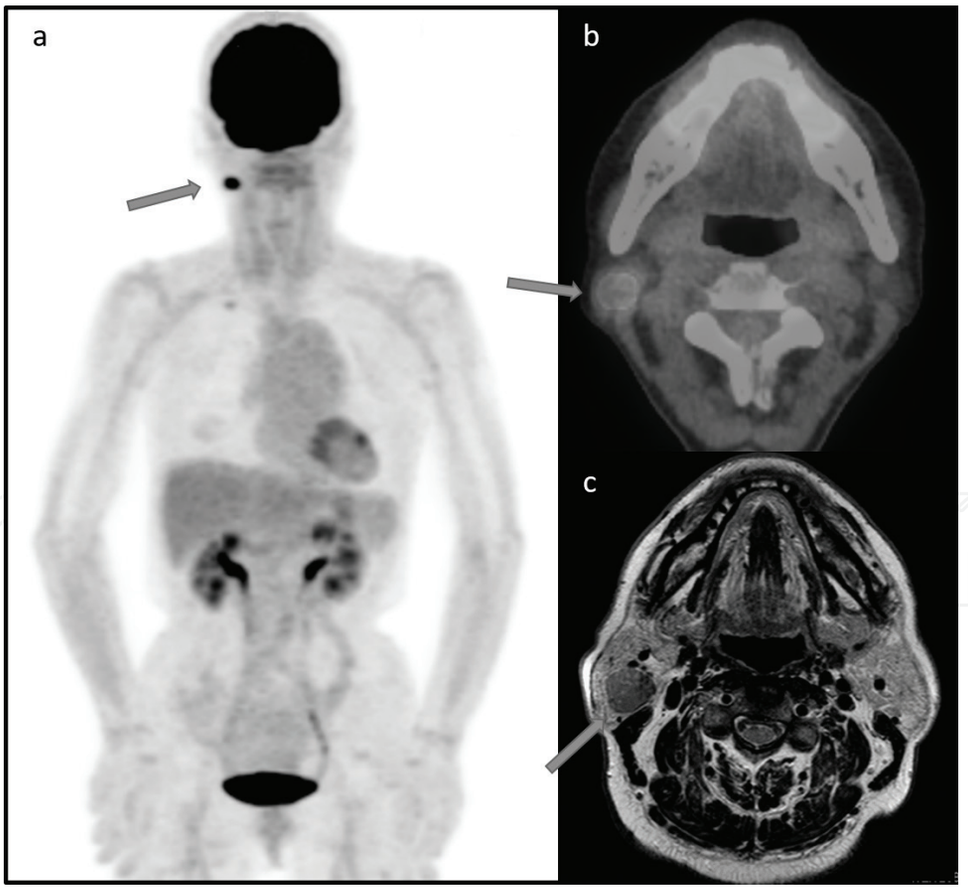

Figure 11. Warthin's tumor. (a). PET MIP image. (b). PET/CT fusion image. (c). T1-weighted MRI image. FDG is strongly taken up by the tumor (SUVmax: 9.4) in the right parotid gland. MRI also provides many findings consistent with malignancy. Salivary gland scintigraphy is useful for differentiation.

http://dx.doi.org/10.5772/intechopen.70622

uptake. Some studies have reported that the differentiation of benign from malignant salivary tumors is possible with the use of indices such as dual-time-point (DTP) imaging and tumor volume, in addition to SUVmax [4, 5].

The sensitivity of PET/CT is approximately 80% for the detection of preoperative primary lesions (**Figure 12**), but the accuracy for staging may vary. In particular, FDG-PET images often show false-positive results for the diagnosis of cervical lymph nodes.

Sialadenitis may show diffuse, increased uptake. However, some cases may show unilateral uptake due to the distribution of inflammation and may be difficult to differentiate from a tumor.

FDG-PET, which provides information about systemic metabolism, is very useful for detecting primary or recurrent lesions for the determination of treatment strategy in cases with highly-malignant tumors requiring aggressive treatment. FDG-PET aids in detection of local involvement, regional lymph node metastasis, distant metastasis, and dissemination for the clinical staging and restaging. It is also useful in the detection of an incidental

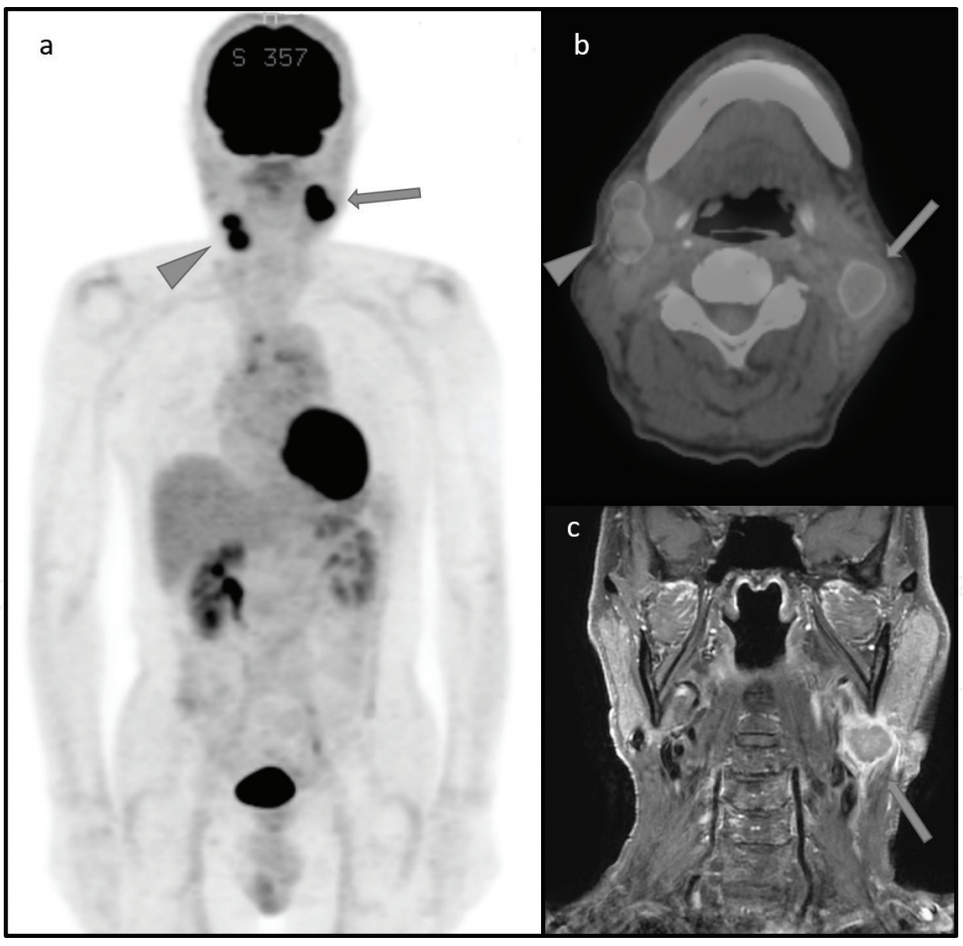

Figure 12. (a). PET MIP image. (b). PET/CT fusion image. (c). T1-weighted MRI using gadolinium-based contrast (GdT1) image. Very strong uptake of FDG (SUVmax: 15.8, arrow) is seen in the region corresponding to the left parotid tumor on the MRI image. Uptake is seen in the region of the right internal jugular lymph nodes (SUVmax: 10.2, arrow head). Parotid cancer or cervical lymph node metastasis is suspected.

cancer. Therefore, this imaging modality is essential before the initiation of treatment and for patient follow-up [4, 5, 13–15].

5. Salivary gland disorders associated with radioiodine therapy

Radioactive iodine (RAI) therapy is the most widely used treatment for differentiated thyroid cancer and has a long history. Because NIS is expressed in the salivary glands, 131I is also incorporated into the salivary glands. Not only thyroid cancer but also salivary glands are irradiated; and thus, acute/chronic sialadenitis may develop.

5.1. Acute salivary gland disorders

Sialadenitis is one of the most common adverse reactions to RAI therapy. Acute-phase sialadenitis causes swelling of the major salivary glands and pain (especially while eating) within one to a few days after oral administration of 131I. Although sialadenitis ameliorates without treatment, xerostomia may develop during the chronic phase and significantly impair the quality of life. Thus, when symptoms develop, sialadenitis should be treated immediately [16, 17]. The parotid glands may be affected more often than the submandibular glands. Steroids are more effective than nonsteroidal anti-inflammatory drugs. Cooling and frequent rinsing with cold water may relieve symptoms. Taste dysfunction is characterized by reduced acuity for salt taste and subsequently sweet taste; bitter taste remains unaffected. Taste dysfunction may become obvious later (2–4 weeks after 131I administration), rather than immediately after administration. To prevent an acute-phase disorder, snacks such as lemon candy to stimulate saliva secretion may be helpful because they also promote the excretion of 131I. Apitherapy using honey products is reportedly useful for preventing salivary gland disorders. Massage of the salivary glands and aroma therapy are also reported to relieve symptoms [18].

5.2. Chronic salivary gland disorders

Xerostomia may develop during the chronic phase, even in patients without acute impairment. Permanent dysfunction is reported to develop more frequently in the submandibular glands than in the parotid glands. Salivary gland scintigraphy shows a pattern of obstructive dysfunction before revealing parenchymal damage of the salivary gland. Therefore, salivary gland function may improve if salivary gland dysfunction can be identified within the period showing an obstructive pattern [19]. Salivary gland function should be monitored regularly with scintigraphy or other studies [20].

6. Conclusions

Radionuclide imaging of salivary glands has been used not only for functional assessment but also for comprehensive diagnosis including morphological information with the advent of single-photon emission computed tomography (SPECT)/CT and PET/CT. Although scientific

evidence is limited, the advantages of radionuclide scanning should be determined. For RAI therapy, attention should be paid to adverse reactions. Coordination among healthcare providers including nurses, radiological technologists, and doctors of all departments involved in treatment is important for achieving effective outcomes.

Acknowledgements

This work was supported by JSPS KAKENHI Grant Number 16K20745.

Author details

Michihiro Nakayama*, Atsutaka Okizaki, Kaori Nakajima and Koji Takahashi

*Address all correspondence to: m-naka@asahikawa-med.ac.jp

Department of Radiology, Asahikawa Medical University, Japan

References

[1] Pilbrow W, et al. Salivary gland scintigraphy–A suitable substitute for sialography? The British Journal of Radiology. 1990;**63**:190-196

[2] Miyake H, et al. Warthin's tumor of parotid gland on Tc-99m pertechnetate scintigraphy with lemon juice stimulation: Tc-99m uptake, size, and pathologic correlation. European Radiology. 2001;**11**:2472-2478

[3] Shizukuishi K, et al. Gland scintigraphy in patients with Sjogren's syndrome. Annals of Nuclear Medicine. 2003;**17**:627-631

[4] Jeong HS, et al. Role of 18 F-FDG PET/CT in management of high-grade salivary gland malignancies. Nuclear-Medizin. 2007;**48**:1237-1244

[5] Nakayama M, et al. Dual-time-point F-18 FDG PET/CT imaging for differentiating the lymph nodes between malignant lymphoma and benign lesions. Annals of Nuclear Medicine. 2013;**27**:163-169. DOI: 10.1007/s12149-012-0669-1

[6] Hadiprodjo D, et al. Parotid gland tumors: Preliminary data for the value of FDG PET/CT diagnostic parameters. AJR. American Journal of Roentgenology. 2012;**198**:W185-W190

[7] Wang HC, et al. Efficacy of conventional whole-body 18F-FDG PET/CT in the incidental findings of parotid masses. Annals of Nuclear Medicine. 2010;**24**:571-577

[8] Blodgett TM, et al. Combined PET-CT in the head and neck: Part 1. Physiologic. Altered physiologic, and artifactual FDG uptake. Radiographies. 2005;**25**:897-912

[9] Lee SK, et al. Parotid incidentaloma identified by combined 18F-fluorodeoxyglucose whole-body positron emission tomography and computed tomography: Findings at grayscale and power Doppler ultrasonography and ultrasound-guided fine-needle aspiration biopsy or core-needle biopsy. European Radiology. 2009;**19**:2268-2274

[10] McGuirt WF, et al. Preoperative identification of benign vs. malignant parotid masses: A comparative study including positron emission tomography. Laryngoscope. 1995;**105**: 579-584

[11] Keyes JW Jr, et al. Salivary gland tumors: Pretherapy evaluation with PET. Radiology 1994;**192**:99-102

[12] Uchida Y, et al. Diagnostic value of FDG PET and salivary gland scintigraphy for parotid tumors. Clinical Nuclear Medicine. 2005;**30**:170-176

[13] Kim KH, et al. The significance of CT scan or MRI in the evaluation of salivary gland tumors. Auris Nasus Larynx. 1998;**25**:397-402

[14] Otsuka H, et al. The impact of FDG-PET in the management of patients with salivary gland malignancy. Annals of Nuclear Medicine. 2005;**19**:691-694

[15] Rob JL, et al. Clinical utility of 18F-FDG PET for patients with salivary gland malignancies. Journal of Nuclear Medicine. 2007;**48**:240-246

[16] Alexander C, Bader JB, Schaefer A, Finke C, Kirsch CM. Intermediate and long-term side effects of high-dose radioiodine therapy for thyroid carcinoma. Journal of Nuclear Medicine. 1998;**39**:1551-1554

[17] Lee SL. Complications of radioactive iodine treatment of thyroid carcinoma. Journal of the National Comprehensive Cancer Network. 2010;**8**:1277-1286

[18] Nakayama M, et al. A randomized controlled trial for the effectiveness of aromatherapy in decreasing salivary gland damage following radioactive iodine therapy for differentiated thyroid cancer. BioMed Research International. 2016;**2016**, Article ID 9509810:6. DOI: 10.1155/2016/9509810

[19] Kim YM, et al. Salivary gland function after sialendoscopy for treatment of chronic radioiodine-induced sialadenitis. Head & Neck. 2016;**38**:51-58

[20] Jeong SY, et al. Salivary gland function 5 years after radioactive iodine ablation in patients with differentiated thyroid cancer: Direct comparison of pre- and postablation scintigraphies and their relation to xerostomia symptoms. Thyroid. 2013;**23**:609-616